Journal of Applied Mechanics and Technical Physics, Vol. 42, No. 4, pp. 572–580, 2001

TURBULENT MIXING OF TWO LIQUIDS WITH AN ARBITRARY LAW OF ACCELERATION

V. E. Neuvazhaev and V. G. Yakovlev

UDC 532.517.4

Based on the $(l$–$v)$ and $(k$–$\varepsilon)$ models, the present paper examines, both numerically and analytically, the turbulent mixing of two liquids of different densities at the interface between them for various laws of their acceleration, namely, constant, decreasing, increasing, and pulsed ones. The numerical results obtained by these models agree well with each other and with experimental data.

INTRODUCTION

The turbulent mixing generated by a shock wave (the Richtmyer–Meshkov instability) was experimentally studied in many works. This phenomenon was also treated theoretically in [1–3]. However, there remain a number of unsolved problems, for instance, those concerning the attainment of the asymptotic flow after the action of the shock wave on the turbulent-mixing zone. It is required to establish whether this flow is a self-similar one. In our opinion, the resultant asymptotic solution is self-similar [1], whereas Shvarts at al. [3] hold quite the opposite point of view. To eliminate the contradictions, an analysis of a simpler situation seems to be helpful. Such a situation was experimentally addressed in [4]. The experiments in [4] were carried out on a setup where an ampoule with two incompressible liquids was accelerated by magnetic forces.

The results of [4] furnish a good test for validating turbulent-mixing models. In this study, four laws of acceleration were considered, namely, constant in time, increasing, decreasing, and triangular ones. The specific features of the setup used in [4] are such that, as the velocity of the ampule increases, a self-similar turbulent-mixing flow is rapidly attained, in contrast, for instance, to the experiments of [5], where initial disturbances were introduced into the flow at the interface between the liquids to avoid a delay in mixing. For some time, such disturbances obviously influence the flow, and this effect should be taken into account when treating experimental data.

The aim of the present work is to compare the previously proposed semi-empirical models [6–8] with the results obtained in [4].

It should be noted that turbulent-mixing regularities were theoretically addressed in [9] for constant, pulsed, power ($g \sim t^m$), and sine laws of acceleration.

1. EQUATIONS OF THE $(k$–$\varepsilon)$ MODEL. COMPARISON WITH EXPERIMENTS

General Equations. To describe the turbulent mixing of liquids in a stationary vessel under a gravity g, a system of equations is used [5], which, for an incompressible liquid, reduces to the following system:

Zababakhin Institute of Technical Physics, Snezhinsk 456770. Translated from Prikladnaya Mekhanika i Tekhnicheskaya Fizika, Vol. 42, No. 4, pp. 11–20, July–August, 2001. Original article submitted August 7, 2000; revision submitted December 8, 2000.

 0021-8944/01/4204-0572 $25.00

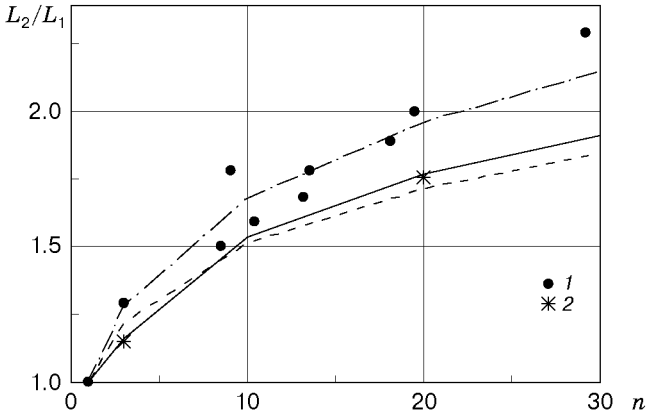

Fig. 1. Turbulent-mixing asymmetry versus the difference in densities: the solid curve refers to the (k–ε) model and the dashed and dot-and-dashed curves refer to $L_2/L_1 = n^{0.18}$ and $n^{0.225}$, respectively; points 1 refer to experimental data of [11, 12] and points 2 refer to experimental data of [5].

$$\frac{dc_i}{dt} = \frac{\partial}{\partial m}\,\rho^2 D_\varepsilon\,\frac{\partial c_i}{\partial m},$$

$$\frac{d\varepsilon_i}{dt} + c_{\varepsilon 2}\,\frac{\varepsilon_t^2}{k} = c_{\varepsilon 1}\hat{g} D_\varepsilon\,\frac{\varepsilon_t}{k}\,\frac{\partial \rho}{\partial m} + \alpha_\varepsilon\,\frac{\partial}{\partial m}\left(\rho^2 D_\varepsilon\,\frac{\partial \varepsilon_t}{\partial m}\right) + \frac{4}{3}\,\varepsilon_t\,\frac{d\rho}{\rho\,dt}, \tag{1.1}$$

$$\frac{dk}{dt} + \varepsilon_t = \hat{g}\,\frac{\partial \rho}{\partial m}\,D_\varepsilon + \alpha_k\,\frac{\partial}{\partial m}\left(\rho^2 D_\varepsilon\,\frac{\partial k}{\partial m}\right) + \frac{2}{3}\,k\,\frac{d\rho}{\rho\,dt},$$

$$\partial m = \rho\,\partial x, \qquad D_\varepsilon = c_\mu\,\frac{k^2}{\varepsilon_t}, \qquad \hat{g} = g(t) + \frac{d}{dt}\,D_\varepsilon\,\frac{\partial \rho}{\partial m}.$$

Here α_ε, α_k, $c_{\varepsilon 1}$, $c_{\varepsilon 2}$, and c_μ are empirical constants, c_i are the mass concentrations of the components (the subscript i denotes respective components), k is the turbulent kinetic energy, ε_t is the rate of dissipation of this energy, D_ε is the turbulent diffusivity, $g(t)$ is a tabulated function, $\rho = \rho_2 n/(c_1 + n(1 - c_1))$ is the density of the mixture, ρ_i are the initial densities of the components, $n = \rho_1/\rho_2$, and $d/dt = \partial/\partial t - D_\varepsilon\,\partial\rho/\partial m(\partial/\partial x)$. At the vessel boundaries, the fluxes of all physical quantities equal zero.

Comparison with the Experiments of [11, 12] and [5] for Constant Acceleration. Figure 1 shows the turbulent-mixing asymmetry as a function of the density ratio n for the case of constant acceleration. The solid curve shows the numerical results obtained by the TURINB computer code [7] (here the penetration depth of the light substance L_1 here was assumed to equal the distance between the interface and the point at which the volume concentration of the light substance was 0.02, and the penetration depth for the heavy substance L_2 was assumed to equal the distance between the interface and the point at which the volume concentration of the light substance was $1 - 0.06/n$). The following values of the parameters involved were used: $\alpha_\varepsilon = 0.85$, $\alpha_k = 0.5$, $c_{\varepsilon 1} = 1.43$, $c_{\varepsilon 2} = 1.85$, and $c_\mu = 3.5$.

Figure 1 also shows the experimental data of [11, 12] and [5]. The difference between the results obtained in these studies is caused by the fact that, in these works, different methods were used to find the mixing front. The experimental data obtained in [11, 12] can be fitted by the curve $L_2/L_1 = n^{0.225}$. The analytical dependence $L_2/L_1 = n^{0.18}$ was obtained by solving self-similar equations. In this case, the position of the mixing front can be determined exactly, the front being not blurred, as it occurs in finite-difference calculations.

If the width of the mixing region is not determined strictly by the front, then, in view of the experimental results obtained in [5], we have

$$\frac{L_2^*}{L_1^*} = (1 + \mathrm{A})^{0.45},$$

where $\mathrm{A} = (\rho_1 - \rho_2)/(\rho_1 + \rho_2)$ is the Atwood number. In the present study, we use this formula, because the width of the mixing region is determined below not by the front but using an integral procedure, which seems to be more reasonable from physical considerations: the limit $\lim\limits_{n\to\infty}(L_2^*/L_1^*)$ is finite. The density profile in [5] was measured in the turbulent-mixing region, which ensures a better reliability of the data on the mixing asymmetry.

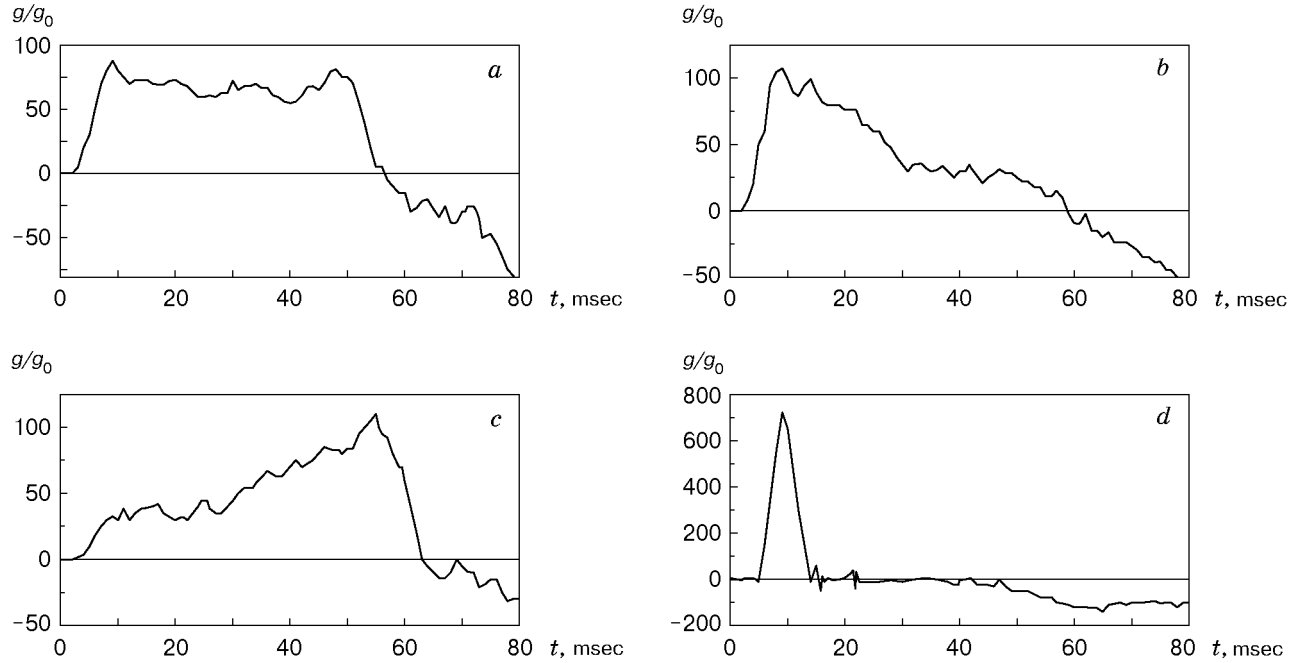

Fig. 2. Dimensionless acceleration g/g_0 versus time ($g_0 = 980$ cm/sec^2): (a) constant acceleration; (b) decreasing acceleration; (c) increasing acceleration; (d) pulsed acceleration.

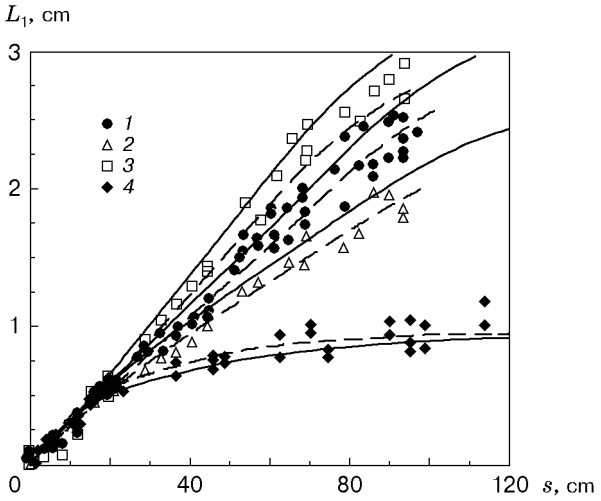

Fig. 3. Comparison between numerical data and the experimental results of [4] ($L_1 = h_b$ and $s = Z$): the solid curves refer to numerical results obtained by the TURINB code and the dashed curves to results obtained by numerical integration of system (3.4), (3.5); the points refer to experimental data for constant acceleration (1), decreasing acceleration (2), increasing acceleration (3), and pulsed acceleration (4).

Comparison with the Experiments of [4]. The experimental results of [4] were modeled using the TURINB code with $\rho_1 = 1$ g/cm^3, $\rho_2 = 1.57$ g/cm^3, and 10-cm layers of the light and heavy liquids. The values of acceleration g were borrowed from [4]; they are shown in Fig. 2. The predicted values compare well with the experimental ones (Fig. 3); in terms of [4], $s = Z = \iint g\,dt'\,dt$.

2. EQUATIONS OF THE (l–v) MODEL IN THE PIECEWISE-CONSTANT TURBULENT DIFFUSIVITY APPROXIMATION

General Equations. In the case of two incompressible liquids that undergo mixing in an ampoule moving with an acceleration g, the equations of the (l–v) model [10] reduce to a system of two equations for the density of the mixture ρ and the turbulent kinetic energy $k = V^2/2$:

$$\frac{\partial \rho}{\partial t} = \frac{\partial}{\partial x}\, D\, \frac{\partial \rho}{\partial x}, \tag{2.1}$$

$$\frac{\partial \rho V^2}{2\partial t} + \frac{\nu \rho D V^2}{\alpha^2 L^2} = Dg\,\frac{\partial \rho}{\partial x} + \frac{4}{3}\,\alpha_3 \rho D\Big[\frac{\partial \ln \rho}{\partial t} - D\Big(\frac{\partial \ln \rho}{\partial x}\Big)^2\Big]^2$$

$$+ \beta_1\,\frac{\partial}{\partial x}\,\rho D\,\frac{\partial V^2}{\partial x} + \frac{D}{2}\,\frac{\partial \ln \rho}{\partial x}\,\frac{\partial \rho V^2}{\partial x} + \frac{5}{6}\,\rho V^2\Big[\frac{\partial \ln \rho}{\partial t} - D\Big(\frac{\partial \ln \rho}{\partial x}\Big)^2\Big]. \tag{2.2}$$

Here $D = \alpha L V$, α, α_3, ν, and β_1 are constants of the model, which should be chosen from the best fit with the experiment, L is the width of the mixing region, and g is the acceleration of the system. The above equations follow from the gas-dynamics equations after their averaging and using the Kolmogorov–Prandtl hypothesis [10].

Approximate Equations. We consider the problem of mixing of two substances with densities ρ_1 at $x > 0$ and ρ_2 at $x < 0$ for a given time-dependent acceleration $g = g(t)$. Under the assumption that the turbulent diffusivity D is a piecewise-constant function with a discontinuity at the point $x = 0$, we may construct the analytical solution

$$D = \begin{cases} \alpha L \bar{V}, & x > 0, \\ \alpha \beta_2 L \bar{V}, & x < 0, \end{cases} \tag{2.3}$$

where $\bar{V}$ is the mean turbulent velocity in the mixing region $[0, L_1]$ and β_2 is an empirical coefficient defined below. In [1, 6], the coefficient β_2 in formula (2.3) was assumed to equal unity, which resulted in mixing symmetry at $L_1 = L_2$.

The approach used in the present study is capable of ensuring the required mixing asymmetry obtained in an experiment (or in a numerical study) through the Atwood number:

$$\sqrt{\beta_2} = (1 + \mathrm{A})^{0.45}. \tag{2.4}$$

Under the above assumption, Eq. (2.1) for the density of the mixture reduces to a linear equation of diffusion with a discontinuous coefficient, and the solution for two incompressible liquids with initial densities ρ_1 and ρ_2 may be expressed through the probability integral $\Phi(\eta)$:

$$\frac{\partial \rho}{\partial \tau} = \begin{cases} \dfrac{\partial^2 \rho}{\partial x^2}, & x > 0, \\ \beta_2\,\dfrac{\partial^2 \rho}{\partial x^2}, & x < 0, \end{cases} \qquad \partial \tau = \alpha L \bar{V}\,\partial t, \qquad \rho = \begin{cases} \rho_0 + (\rho_1 - \rho_0)\Phi(\eta), & \eta > 0, \\ \rho_0 + (\rho_0 - \rho_2)\Phi(\eta), & \eta < 0, \end{cases}$$

$$\rho_0 = \frac{\rho_1 + \rho_2\sqrt{\beta_2}}{1 + \sqrt{\beta_2}}, \quad \Phi = \frac{2}{\sqrt{\pi}}\int\limits_0^{\eta} \mathrm{e}^{-z^2}\,dz, \quad \eta = \begin{cases} x/(2\sqrt{\tau}\,), & x > 0, \\ x/(2\sqrt{\beta_2 \tau}\,), & x < 0. \end{cases} \tag{2.5}$$

Solution (2.5) has no distinct front from which it would be possible to determine the mixing-region width. Therefore, to find the turbulent-mixing front, we introduce the volume concentrations $f_1 = (\rho - \rho_2)/(\rho_1 - \rho_2)$ and $f_2 = (\rho_1 - \rho)/(\rho_1 - \rho_2)$. With the parameters f_1 and f_2, as in [1], we suggest using the integral procedure for determining the widths L_1^* and L_2^*:

$$L_2^* = 2\int\limits_{-\infty}^{0} \frac{f_1\,dx}{f_1(0)}, \qquad L_1^* = 2\int\limits_{0}^{\infty} \frac{f_2\,dx}{f_2(0)}.$$

Using solution (2.5), we have

$$L_1 = 2\eta_1\sqrt{\tau}, \qquad L_2 = 2\eta_1\sqrt{\beta_2\tau}, \qquad \eta_1 = 2/\sqrt{\pi}. \tag{2.6}$$

From here on, the superscript asterisk is omitted.

It only remains to derive the equation for the mean turbulent velocity $\bar{V}(t)$. We average Eq. (2.2) over the entire mixing region $-L_2 \leqslant x \leqslant L_1$. Instead of the coefficient D, we use its value (2.3) and pass from t to τ. After averaging over the region $-L_2 \leqslant x \leqslant L_1$, we obtain the equation

$$\frac{d(\bar{V}^2 M)}{2d\tau} + \frac{\nu\bar{V}^2 M}{\alpha^2 L^2}\,\frac{1+\beta_2^{3/2}}{1+\sqrt{\beta_2}}$$

$$= \bar{g}\Phi(\eta_1)\sqrt{\beta_2}(\rho_1-\rho_2) + \frac{1}{3}\,\alpha_3\alpha_1^2\eta_1^4\,\mathrm{A}_0^4\,X_0\,\frac{\bar{V}^2 M}{\tau} - \frac{\Phi(\sqrt{2}\eta_1)}{12\sqrt{2}}\,\mathrm{A}_0^2\,X_p\,\frac{\bar{V}^2 M}{\tau},$$

where

$$X_0 = \frac{1+\sqrt{\beta_2}}{2}\Big[\sqrt{\beta_2}+\beta_2^2+\frac{3}{2}\,\mathrm{A}_0\,\eta_1^2\sqrt{\beta_2}\,(1-\beta_2^2)\Big], \quad M = \rho_0 L, \quad \mathrm{A}_0 = \frac{\rho_1-\rho_2}{\rho_1+\rho_2\sqrt{\beta_2}},$$

$$X_p = \left[1 - \frac{\mathrm{A}_0\,\sqrt{2}(\sqrt{\beta_2}-1)\eta_1^2}{4\Phi(\sqrt{2}\,\eta_1)}\right]\sqrt{\beta_2}.$$

The bar denotes averaging over the mixing region $[-L_2, L_1]$. The relation between the width L and the variable τ is known from (2.6). Finally, we obtain the following equations for the unknown functions $\bar{V}^2$ and L:

$$\frac{d\bar{V}^2}{dL} + 4k_y\,\frac{\bar{V}^2}{L} = \frac{\Phi(\eta_1)\sqrt{\beta_2}}{\eta_1^2(1+\sqrt{\beta_2})}\,\bar{g}\,\mathrm{A}_0,$$

$$\frac{dL}{dt} = 2\alpha\eta_1^2(1+\sqrt{\beta_2}\,)^2\bar{V}, \qquad L = L_1+L_2 = 2\eta_1(1+\sqrt{\beta_2}\,)\sqrt{\tau}, \tag{2.7}$$

$$4k_y = 1 + \frac{\nu(1+\beta_2^{3/2})}{(1+\sqrt{\beta_2}\,)^3\eta_1^2\alpha^2} + \frac{\Phi(\sqrt{2}\,\eta_1)}{3\sqrt{2}}\,\mathrm{A}_0^2 X_p - \frac{4\alpha_3\alpha^2\eta_1^4}{3}\,\mathrm{A}_0^4 X_0.$$

In derivation of Eqs. (2.7), we used the equality $L = 2(1+\sqrt{\beta_2}\,)\eta_1\sqrt{\tau}$.

Allowance for Additional Acceleration. Choice of Model Constants. The developing turbulent mixing gives rise to a flow of the substance with a velocity $u = -D\partial\ln\rho/\partial x$. We average this relation over the mixing region $-L_2 \leqslant x \leqslant L_1$ after multiplying both parts of the equality by ρ. We have $\bar{u} = -\alpha L\bar{V}(\rho_1-\rho_2)\Phi(\eta_1)\sqrt{\beta_2}/M = -\alpha\sqrt{\beta_2}(1+\sqrt{\beta_2}\,)\,\mathrm{A}_0\bar{V}\Phi(\eta_1)$. The flow arising in this situation causes the interface move, which involves additional acceleration

$$\bar{g}_1 = \bar{g} + \frac{\partial\bar{u}}{\partial t} \approx \bar{g} - \alpha(1+\sqrt{\beta_2})\sqrt{\beta_2}\,\mathrm{A}_0\Phi(\eta_1)\frac{\partial\bar{V}}{\partial t}. \tag{2.8}$$

The additional acceleration should be taken into account when calculating the generation term in Eq. (2.7) for the turbulent kinetic energy. To this end, in the first equation of (2.7), the acceleration $\bar{g}$ should be substituted, according to (2.8), by $\bar{g}_1$. This substitution results in a change in the coefficient at the derivative $d\bar{V}^2/dL$:

$$Z_0\,\frac{d\bar{V}^2}{dL} + 4k_y\,\frac{\bar{V}^2}{L} = \frac{\Phi(\eta_1)\sqrt{\beta_2}}{\eta_1^2(1+\sqrt{\beta_2})}\,\bar{g}\,\mathrm{A}_0, \quad Z_0 = 1+\alpha^2\beta_2(1+\sqrt{\beta_2}\,)^2\mathrm{A}_0^2\Phi^2(\eta_1). \tag{2.9}$$

The equation thus obtained is linear with respect to the function $\bar{V}^2$ and may be integrated for an arbitrary time-dependent acceleration $\bar{g}$.

The model includes three constants, namely, α, α_2, and ν. Let us choose their values. We consider the case of small Atwood numbers A_0; in this case, we may use the substitution $k_y \approx k_0 = 0.25 + \nu/(16\eta_1^2\alpha^2)$ in the coefficients entering Eq. (2.9) and set the acceleration in the form of a piecewise-constant function

$$\bar{g} = \begin{cases} g_0, & 0 \leqslant t \leqslant t_0, \\ 0, & t > t_0. \end{cases}$$

Under the above assumptions, the solution of Eq. (2.9) can be obtained in the analytical form [1]:

$$L_1 = \begin{cases} \dfrac{4\alpha^2\eta_1^2\Phi(\eta_1)g_0\,\mathrm{A}_0\,t^2}{1+4k_0}, & 0 \leqslant t \leqslant t_0, \\ L_{10}\Big(1+\dfrac{2}{B_0}\,\dfrac{t-t_0}{t_0}\Big)^{B_0}, & t > t_0. \end{cases} \tag{2.10}$$

Here $L_{10} = 4\alpha^2\eta_1^2\Phi(\eta_1)g_0t_0\mathrm{A}_0/(1+4k_0)$ and $B_0 = 1/(1+2k_0)$.

In integration, we used the condition $\bar{V}_0 = L_0 = 0$ for $t = 0$. The theory [6] and the experiment [5] for $\mathrm{A} = 0$ yield $B_0 = 2/7$; hence, $k_0 = 1.25$ or $\nu/(16\eta_1^2\alpha^2) = 1$. Here, we took into account that $\sqrt{\beta_2}$ depends on A according to (2.4) and $\beta_2 = 1$ for $\mathrm{A} = 0$. Following [5, 11, 12], we choose the constant α from the condition $L_1 = 0.06g_0\,\mathrm{A}\,t^2$. We put the constant α_3 to equal unity. Taking into account that $\eta_1 = 1.128$, $\Phi(\eta_1) = 0.89$, and $\Phi(\sqrt{2}\,\eta_1) = 0.97$, we finally obtain $\alpha = 0.282$, $\alpha_3 = 1$, and $\nu = 1.62$. Obviously, the role played by the constant $\alpha_3 = 1$ is insignificant; therefore, we put $\alpha_3 = 0$ for simplicity.

Analytical Solution for Constant and Pulsed Accelerations and for an Arbitrary Atwood Number. Let us integrate Eq. (2.9). For constant acceleration and zero initial conditions, Eq. (2.9) and the equation for the mixing-region width in (2.7) yield the following solution:

$$\frac{L_1}{2s} = J_1 = \frac{\alpha^2\eta_1^2(1+\sqrt{\beta_2})^2\sqrt{\beta_2}\Phi(\eta_1)\mathrm{A}_0}{Z_0 + 4k_y}. \tag{2.11}$$

The solution for pulsed acceleration in the general case, in which $L_0(0) \neq 0$, can be obtained by introducing the dimensionless parameter $\beta = U_0t_0/L_0$. Then, the solution for the total width results from integration of Eqs. (2.9) and the second equation in (2.7). The action of pulsed acceleration results in the fact that, for an initial roughness $L_0 \neq 0$, $\bar{V}_1(\beta)$ and L_{10} assume the following values for the time t_0:

$$\bar{V}_1(\beta) = U_0\sqrt{\frac{\tilde{\mathrm{A}}\,\Phi(\eta_1)}{2\eta_1^2(1+4\tilde{k}_y)\beta}\,\frac{L_{10}}{L_0}\left[1-\Big(\frac{L_{10}}{L_0}\Big)^{-(1+\tilde{k}_y)}\right]},$$

$$\sqrt{\frac{L_{10}}{L_0}} = \begin{cases} \sqrt{1+8\eta_1^2\tilde{\alpha}^2\Phi(\eta_1)\tilde{\mathrm{A}}\,\beta} & \text{for} \quad \beta\tilde{\mathrm{A}} < \dfrac{1}{32\tilde{k}_y\eta_1^2\alpha^2\Phi(\eta_1)}, \\ \sqrt{\dfrac{4\tilde{k}_y}{1+4\tilde{k}_y}} + 4\eta_1\tilde{\alpha}\sqrt{\dfrac{\Phi(\eta_1)\tilde{\mathrm{A}}\,\beta}{2(1+4\tilde{k}_y)}} & \text{for} \quad \beta\tilde{\mathrm{A}} \geqslant \dfrac{1}{32\tilde{k}_y\eta_1^2\alpha^2\Phi(\eta_1)}. \end{cases} \tag{2.12}$$

Here $\tilde{\mathrm{A}} = 2\,\mathrm{A}_0(1+\sqrt{\beta_2})/Z_0$, $\tilde{k}_y = k_y/Z_0$, and $\tilde{\alpha} = \alpha(1+\sqrt{\beta_2})^2/4$. In deriving (2.12), we used the following approximate representation of the solution:

$$\frac{\bar{V}}{U_0} = \begin{cases} \sqrt{\dfrac{\Phi(\eta_1)}{2\eta_1^2}\,\beta\tilde{\mathrm{A}}\Big(\dfrac{L}{L_0}-1\Big)}, & \dfrac{L}{L_0} < \dfrac{1+4\tilde{k}_y}{4\tilde{k}_y}, \\ \sqrt{\dfrac{\Phi(\eta_1)\beta\tilde{\mathrm{A}}}{2\eta_1^2(1+4\tilde{k}_y)}\,\dfrac{L}{L_0}}, & \dfrac{L}{L_0} \geqslant \dfrac{1+4\tilde{k}_y}{4\tilde{k}_y}. \end{cases}$$

After the action of pulsed acceleration, the solution is given by the formulas $\bar{V} = (L_{10}/L)^{(1-B)/B}\bar{V}_1(\beta)$,

$$L = L_{10}\left[1+2\eta_1^2\alpha\,\frac{(1+\sqrt{\beta_2})^2}{BL_{10}}\,\tilde{V}_1(\beta)(t-t_0)\right]^B; \tag{2.13}$$

$$B = Z_0/(Z_0+2k_y). \tag{2.14}$$

Formulas (2.11) and (2.14) describe the dependence of the intensity J_1 and power exponent B on the Atwood number A. These dependences are shown in Fig. 4. Roughly, they may be expressed by the following simple formulas

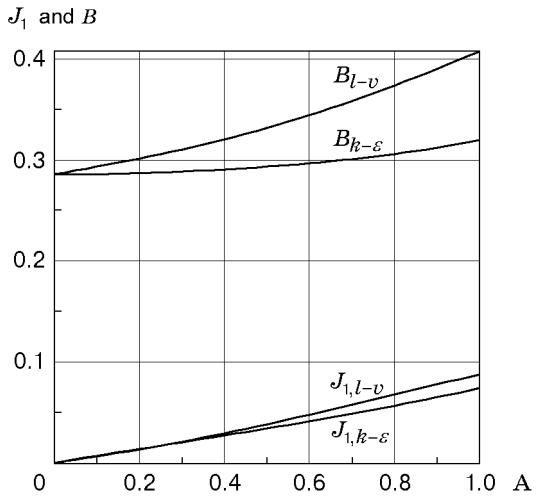

Fig. 4. Intensities $J_{1,k-\varepsilon}$ and $J_{1,l-v}$ and degrees of decay $B_{k-\varepsilon}$ and B_{l-v} of turbulent mixing versus the Atwood number A in the (l–v) and (k–ε) models.

$$\frac{dL_1}{2ds} = J_1 = 0.06(1 + 0.61\,\mathrm{A})\,\mathrm{A}, \qquad B = \frac{2}{7} + 0.09\,\mathrm{A}^2. \tag{2.15}$$

Thus, the widely-used linear dependence $J_1(\mathrm{A})$ is valid only in a vicinity of small values of A. Therefore, in using this dependence in the limiting case $\mathrm{A} = 1$, one has to multiply the coefficient α by a factor of 1.61. With increasing Atwood number, in the (l–v) model, the power exponent B also increases from 0.28 to 0.38.

Solution for Arbitrary Acceleration (Comparison with the Results of [4]). For arbitrary acceleration, Eq. (2.9) and the second equation in (2.7) can be integrated numerically. In the case of pulsed acceleration, the solution is given by formula (2.13). For the initial conditions $U_0 = 3.4$ cm/msec, $L_{10} = 0.4$ cm, $t_0 = 9$ msec, and $\mathrm{A} = 0.22$, we have $L_1 = 0.4[1 + 0.786(t - 9)]^{0.288}$ cm.

It should be noted that the mixing-region width L_{10} at the moment the acceleration stops acting coincides with the measured one. The latter means that, in the experiment, random initial disturbances of small amplitude occurred at the initial moment, so that the initial roughness L_0 could be neglected, compared to the width L_{10} obtained after the action of pulsed acceleration. An estimate of L_{10} results from (2.12) under the assumption of high values of the parameter β ($\beta \to \infty$):

$$\sqrt{L_{10}} = 4\eta_1\tilde{\alpha}\sqrt{\frac{\Phi(\eta_1)\tilde{\mathrm{A}}U_0 t_0}{2(1 + 4\tilde{k}_y)}}.$$

Equation (2.9) and the second equation in (2.7) for small Atwood numbers are identical to Eqs. (1) in [4]:

$$\frac{dV_b^2}{dh_b} = \beta_0\,\mathrm{A}\,g - C_d\,\frac{V_b^2}{h_b}, \qquad \frac{dh_b}{dt} = V_b. \tag{2.16}$$

Here $h_b = L_1$ and $V_b = 1.5\bar{V}$. The choice of the constants β_0 and C_d in the present study differs from that in [4]: $\beta_0 = 0.73$ (instead of 0.5 in [4]) and $C_d = 2.3$ (instead of 1.6 in [4]).

Note also that, unlike the equation obtained in [4] [Eq. (2.16) in this work], the resultant equation (2.9) is more general, since it establishes an additional dependence of the solution on the Atwood number. Equations (2.16) for the mixing intensity J_1 yield the formula $J_1 = 0.06\mathrm{A}$, whereas law (2.15) follows from (2.9).

3. EQUATIONS OF THE (k–ε) MODEL IN THE PIECEWISE-CONSTANT DIFFUSIVITY APPROXIMATION

The piecewise-constant diffusivity approximation may be also applied to the equations arising in the (k–ε) model [1]:

$$D_\varepsilon = \begin{cases} c_\mu \bar{k}^2/\bar{\varepsilon}_t, & x > 0, \\ c_\mu \beta_2 \bar{k}^2/\bar{\varepsilon}_t, & x < 0. \end{cases} \tag{3.1}$$

Here β_2 is the coefficient that can be determined empirically using formula (2.4); the turbulent energy $\bar{k}$ and the intensity $\bar{\varepsilon}_t$ are functions of time only. On averaging the initial equations of model (1.1) over the mixing region $-L_2 \leqslant x \leqslant L_1$, we obtain

$$\frac{d\bar{k}}{dL^2} - P_0\,\frac{\bar{k}}{L^2} + \frac{\bar{\varepsilon}_t^2}{4\eta_1^2(1+\sqrt{\beta_2}\,)^2 c_\mu \bar{k}^2} = \frac{\Phi(\eta_1)\sqrt{\beta_2}\,\bar{g}\,\mathrm{A}_0}{4\eta_1^2 L(1+\sqrt{\beta_2})},$$

$$\frac{d\bar{\varepsilon}_t}{dL^2} - P_2\,\frac{\bar{\varepsilon}_t}{L^2} + \frac{c_{\varepsilon 2}\bar{\varepsilon}_t^3}{4\eta_1^2(1+\sqrt{\beta_2}\,)^2 c_\mu \bar{k}^3} = \frac{\Phi(\eta_1)\sqrt{\beta_2}\,c_{\varepsilon_1}\bar{g}\,\mathrm{A}_0\bar{\varepsilon}_t}{\eta_1^2 L\bar{k}(1+\sqrt{\beta_2}\,)}, \tag{3.2}$$

$$\frac{dL^2}{dt} = 4\eta_1^2 c_\mu (1+\sqrt{\beta_2})^2\,\frac{\bar{k}^2}{\bar{\varepsilon}_t},$$

where $P_0 = -0.5 - 1/(6\sqrt{2}\,)\Phi(\sqrt{2}\eta_1)\,\mathrm{A}_0^2 X_p$ and $P_2 = -0.5 - 1/(3\sqrt{2}\,)\Phi(\sqrt{2}\eta_1)\,\mathrm{A}_0^2 X_p$. To simplify the equations thus obtained, we adopt one more assumption [13], namely, we put the model constant $c_{\varepsilon 1}$ equal to 1.5 instead of 1.43 in the general model. In this case, equations of model (3.2) admit the integral

$$\bar{\varepsilon}_t^2 = 4\eta_1^2 \tilde{c}_\mu\,\frac{18-\sqrt{2}\Phi(\sqrt{2}\eta_1)\mathrm{A}_0^2 X_p}{3(2c_{\varepsilon 2}-3)}\,\frac{\bar{k}^3}{L^2}, \tag{3.3}$$

where $\tilde{c}_\mu = c_\mu(1+\sqrt{\beta_2}\,)^2/4$ and $\tilde{\mathrm{A}}_0 = 2\,\mathrm{A}_0/(1+\sqrt{\beta_2}\,)$.

In view of (3.3), Eqs. (3.2) may be written as

$$\theta_0\,\frac{d\bar{k}}{dL} + 2P_3\,\frac{\bar{k}}{L} = \frac{\Phi(\eta_1)\sqrt{\beta_2}g_0\tilde{\mathrm{A}}_0}{4\eta_1^2}, \tag{3.4}$$

$$\frac{dL}{dt} = 8\eta_1\sqrt{\tilde{c}_\mu \bar{k}}\sqrt{\frac{3(2c_{\varepsilon 2}-3)}{18-\sqrt{2}\Phi(\sqrt{2}\eta_1)\mathrm{A}_0^2 X_p}}, \tag{3.5}$$

where

$$\theta_0 = 1 + \frac{3(2c_{\varepsilon 2}-3)c_\mu \Phi^2(\eta_1)\sqrt{\beta_2}\,\mathrm{A}_0^2}{\eta_1^2(18-\sqrt{2}\Phi(\sqrt{2}\eta_1)\,\mathrm{A}_0^2 X_p)}, \qquad P_3 = -P_0 + \frac{18-\sqrt{2}\Phi(\sqrt{2}\eta_1)\,\mathrm{A}_0^2 X_p}{12(2c_{\varepsilon 2}-3)}.$$

Here, the additional acceleration

$$\frac{d\bar{u}}{dt} = -2c_\mu\sqrt{\beta_2}(1+\sqrt{\beta_2}\,)\frac{3(2c_{\varepsilon 2}-3)\Phi(\eta_1)\,\mathrm{A}_0}{18-\sqrt{2}\Phi(\sqrt{2}\eta_1)\,\mathrm{A}_0^2 X_p}\,\frac{d\bar{k}}{dL}$$

is taken into account, which should be added to the acceleration $\bar{g}$ in the right-hand part of the first equation in (3.2).

With $\bar{k} = \bar{V}^2/2$, Eq. (3.4) for small A_0 becomes equivalent to (2.9). With $\alpha_\varepsilon = 0.85$, $c_\mu = 1.62$, $c_{\varepsilon 2} = 15/8$, $\eta_1 = 1.128$, $\Phi(\eta_1) = 0.89$, and $\Phi(\sqrt{2}\,\eta_1) = 0.97$, Eqs. (3.5) and (2.7) for the mixing-region width become identical to each other for small A_0 and consistent with formula (2.10) ($0 \leqslant t \leqslant t_0$). However, if A_0 is not small, other dependences, different from (2.15), arise in the (k–ε) model (see Fig. 3).

The intensity J_1 and the power exponent B depend on the Atwood number as follows: $dL_1/2ds = J_1 = 0.06(1+0.42\mathrm{A})\mathrm{A}$ and $B = 2/7 + 0.05\mathrm{A}^2$. A comparison between the intensity J_1 and the degree of decay B of turbulent mixing predicted by the (l–v) and (k–ε) models is shown in Fig. 3. The intensities $J_{1,k-\varepsilon}$ and $J_{1,l-v}$ are almost coincident for small A; however, for $A = 1$, we have $J_{1,k-\varepsilon}/J_{1,l-v} = 1.14$. The value of B increases with the Atwood number in both models but more slowly in the (k–ε) model. As a result, $B_{l-v}/B_{k-\varepsilon} = 1.12$ for $\mathrm{A} = 1$. To clarify the reason for the above differences, additional experiments are necessary.

The results of integration of system (3.4) and (3.5) for four types of acceleration and $\mathrm{A} = 0.22$ are shown in Fig. 3. A comparison of these results reveals a good correlation with the experimental data of [4], which validates the approximate model.

CONCLUSIONS

With the use of the (k–ε) model, development of the turbulent-mixing region is considered for four types of acceleration, namely, constant, decreasing, increasing, and pulsed ones. The numerical results obtained with the help of the TURINB computer code agree well with the experimental data of [4].

In the piecewise-constant turbulent diffusivity approximation, analytical solutions are constructed for constant and pulsed acceleration, and also for four types of acceleration from [4]. In the (l–v) and (k–ε) models, simple analytical expressions that describe the turbulent-mixing intensity $dL_1/2ds$ and the degree of decay B as functions of the Atwood number are derived. There is a certain discrepancy between the two models, and available experimental data do not permit the final decision between them.

The results obtained by the exact (k–ε) model and the approximate (l–v) and (k–ε) models are compared with the experimental data of [4]. The comparison show a good correlation between the experiment and the theory, which justifies the previously made choice of constants in the (k–ε) and (l–v) models, and provides support for the approximate formulas proposed. Of obvious interest is a similar comparison for other known semi-empirical models.

The authors are grateful to A. V. Polionov for useful comments on the work.

REFERENCES

1. V. E. Neuvazhaev, "Development of turbulent mixing caused by Richtmyer–Meshkov instability," *Mat. Model.*, **3**, No. 7, 10–28 (1991).
2. K. Mikaelian, "Turbulent mixing generated by Rayleigh–Taylor and Richtmyer–Meshkov instabilities," *Physica D*, **36**, 343–348 (1989).
3. D. Shvarts, U. Alon, D. Ofer, et al., "Nonlinear evolution of multimode Rayleigh–Taylor instability in two and three dimensions," *Phys. Plasmas*, **2**, 2465–2472 (1995).
4. G. Dimontea and M. Schneider, "Turbulent Rayleigh–Taylor instability experiments with variable acceleration," *Phys. Rev. E*, **54**, No. 4, 3740–3743 (1996).
5. Yu. A. Kucherenko, S. I. Balabin, A. P. Pylaev, et al., "Experimental study of the gravitational turbulent mixing self-similar mode," in: *Proc. of the 3rd Int. Workshop on the Physics of Compressible Turbulent Mixing* (Abbey of Royamont, France, June 17–19, 1991), S. l, pp. 427–454.
6. V. E. Neuvazhaev, "On the turbulent-mixing theory," *Dokl. Akad. Nauk SSSR*, **222**, No. 5, 1053–1056 (1975).
7. V. E. Neuvazhaev and V. G. Yakovlev, "Predicting of turbulent mixing under gravity by the (k–ε) model," in: *Questions of Atomic Science and Engineering*, *Ser. Theoretical and Applied Physics*, No. 1 (1988), pp. 28–36.
8. V. E. Neuvazhayev, "Turbulent mixing induced by the Richtmyer–Meshkov instability," in: *Proc. of the 3rd Int. Workshop on the Physics of Compressible Turbulent Mixing* (Abbey of Royamont, France, June 17–19, 1991), S. l, pp. 483–494.
9. V. E. Neuvazhaev, "Properties of the model of turbulent mixing of the interface between accelerated liquids of different densities," *Prikl. Mekh. Tekh. Fiz.*, No. 5, 81–88 (1983).
10. V. E. Neuvazhaev and V. G. Yakovlev, "A model and method for numerical simulation of the turbulent mixing of an interface moving with an acceleration," in: *Questions of Atomic Science and Engineering*, *Ser. Techniques and Programs for Solving Problems of Mathematical Physics*, No. 2 (1984), pp. 17–25.
11. D. L. Youngs, "Numerical simulation of turbulent mixing by Rayleigh–Taylor instability," *Physica D*, **12**, 32–44 (1984).
12. K. I. Read, "Experimental investigation of turbulent mixing by Rayleigh–Taylor instability," *ibid.*, pp. 45–57.
13. V. E. Neuvazhaev, "Some properties of the turbulent-mixing model based on the two-component, two-velocity model. Separation additive in diffusion models," *Mat. Model.*, **7**, No. 7, 3–18 (1995).